

# The pivotal role of the $\beta 7$ strand in the intersubunit contacts of different human small heat shock proteins

Evgeny V. Mymrikov · Olesya V. Bukach ·  
Alim S. Seit-Nebi · Nikolai B. Gusev

Received: 26 August 2009 / Revised: 1 October 2009 / Accepted: 12 October 2009 / Published online: 24 October 2009  
© Cell Stress Society International 2009

**Abstract** Human  $\alpha$ B-crystallin and small heat shock proteins HspB6 and HspB8 were mutated so that all endogenous Cys residues were replaced by Ser and the single Cys residue was inserted in a position homologous to that of Cys137 of human HspB1, i.e. in a position presumably located in the central part of  $\beta 7$  strand of the  $\alpha$ -crystallin domain. The secondary, tertiary, and quaternary structures of thus obtained Cys-mutants as well as their chaperone-like activity were similar to those of their wild-type counterparts. Mild oxidation of Cys-mutants leads to formation of disulfide bond crosslinking neighboring monomers thus indicating participation of the  $\beta 7$  strand in intersubunit interaction. Oxidation weakly affects the secondary and tertiary structure, does not affect the quaternary structure of  $\alpha$ B-crystallin and HspB6, and shifts equilibrium between monomer and dimer of HspB8 towards dimer formation. It is concluded that the  $\beta 7$  strand participates in the intersubunit interaction of four human small heat shock proteins ( $\alpha$ B-crystallin, HspB1, HspB6, HspB8) having different structure of  $\beta 2$  strand of  $\alpha$ -crystallin domain and different length and composition of variable N- and C-terminal tails.

**Keywords** Small heat shock proteins · Oligomeric structure · Intersubunit contacts

**Electronic supplementary material** The online version of this article (doi:10.1007/s12192-009-0151-8) contains supplementary material, which is available to authorized users.

E. V. Mymrikov · O. V. Bukach · A. S. Seit-Nebi ·  
N. B. Gusev (✉)  
Department of Biochemistry, School of Biology,  
Moscow State University,  
Moscow 119991, Russian Federation  
e-mail: NBGusev@mail.ru

## Abbreviations

Cys-mutant of $\alpha$ B-crystallin	Human $\alpha$ B-crystallin with point mutation E117C
Cys-mutant of HspB6	Human HspB6 with double mutation C46S/E116C
Cys-mutant of HspB8	Human HspB8 with fourfold mutation C10S/C99S/C195S/N138C
bis-ANS	4,4'-Bis(1-anilinonaphthalene-8-sulfonate)
DTT	Dithiothreitol
ME	$\beta$ -Mercaptoethanol
PMSF	Phenylmethanesulfonyl fluoride
sHsp	Small heat shock proteins

## Introduction

The family of small heat shock proteins combines a wide number of members that are expressed throughout all kingdoms, except for some pathogenic bacteria (Haslbeck et al. 2005). The molecular mass of small heat shock proteins varies in the range of 12–43 kDa and these proteins contain conservative  $\alpha$ -crystallin domain containing 70–80 residues flanked by comparatively short and variable N- and C-terminal tails (Haslbeck et al. 2005; Vos et al. 2008; Mchaourab et al. 2009). Small heat shock proteins tend to form mobile oligomers of different size and compositions (Haley et al. 2000; Vos et al. 2008; Mchaourab et al. 2009).

The human genome contains 11 genes encoding different small heat shock proteins which are denoted HspB1–HspB11 and have different molecular masses which are also used for their designation (for instance, Hsp20, Hsp22, or Hsp27; Vos et al. 2008). Some members of the human sHsp family are tissue-specific (e.g., HspB9 and HspB10),

whereas others are ubiquitously expressed in practically all tissues (e.g., HspB1 (Hsp27), HspB6 (Hsp20), HspB8 (Hsp22), and HspB5 ( $\alpha$ B-crystallin); Vos et al. 2008; Taylor and Benjamin 2005). Small heat shock proteins seem to play an important house-keeping role in the cell and prevent accumulation of aggregates of partially denatured proteins (Vos et al. 2008; Mchaourab et al. 2009; Ecroyd and Carver 2009), participate in regulation of cytoskeleton (Mounier and Arrigo 2002), and seem to be involved in regulation of proliferation and apoptosis (Arrigo et al. 2007). Since sHsp are involved in diverse cellular processes, mutations of these proteins often correlate with development of different congenital diseases (Sun and MacRae 2005; Benndorf and Welsh 2004) and sHsp are considered important therapeutic targets (Arrigo et al. 2007).

The structural information is important for understanding the mechanism of sHsp functioning. However, high mobility, different size, and variable oligomeric state complicate investigation of sHsp structure. Up until now, the structure of only three sHsp, namely *Methanococcus jannaschii* Hsp16.5 (Kim et al. 1998), wheat *Triticum aestivum* Hsp16.9 (van Monfort et al. 2001) and Tsp36 of parasitic flatworm *Taenia saginata* (Stamler et al. 2005) was described in the literature. Although the primary structure of human sHsp is similar to that of sHsp isolated from other species, there are certain important differences both in the conserved  $\alpha$ -crystallin domain and in the variable N- and C-terminal ends (van Monfort et al. 2001; Mchaourab et al. 2009; Kasakov et al. 2007; Michiel et al. 2009). This complicates direct comparison of the structure of already crystallized sHsp (Kim et al. 1998; van Monfort et al. 2001; Stamler et al. 2005) with their human counterparts. To overcome this problem, cryo-electron microscopy (Haley et al. 2000), site-directed spin labeling (Mchaourab et al. 2009; Berengian et al. 1999), and protein pin array technique (Ghosh and Clark, 2005) were used for investigation of the structure of full-size human sHsp. In addition, the structure of isolated  $\alpha$ -crystallin domain of human sHsp was analyzed by means of hybrid solid-solution NMR spectroscopy (Jehle et al. 2009), synchrotron radiation X-ray scattering (Feil et al. 2001), and X-ray crystallography (Bagneris et al. 2009).

The data obtained on isolated  $\alpha$ -crystallin domains cannot be unequivocally used for describing the structure of full-size proteins. Moreover, there are large differences even in the structure of isolated  $\alpha$ -crystallin domains determined by different methods (Feil et al. 2001; Jehle et al. 2009; Bagneris et al. 2009) and significant differences in the detail of dimer structure of crystallin domains derived from different sHsp (Bagneris et al. 2009). Finally, the data obtained up to now predominantly illuminate structural properties of human  $\alpha$ B-crystallin (HspB5) and to a smaller

extent of HspB1 and HspB6. At the same time, the members of human sHsp family have a rather diverse structure of both  $\alpha$ B-crystallin domain and of variable N- and C-terminal ends (Stamler et al. 2005; Kasakov et al. 2007; Bagneris et al. 2009). This makes desirable systematic investigation of intersubunit interaction of different full size human sHsp.

We supposed that the  $\beta$ 7-strand of the  $\alpha$ -crystallin domain plays important role in intersubunit interaction of different human sHsp. The earlier published data indicate that the mouse Hsp25 containing the single Cys residue (Cys141) homologous to that of Cys137 of human HspB1 and located in the  $\beta$ 7-strand easily forms intersubunit disulfide bond (Zavialov et al. 1998a). Moreover, this residue is easily accessible for thiol-disulfide exchange (Zavialov et al. 1998b) and undergoes S-thiolation under oxidative conditions (Eaton et al. 2002). We supposed that the introduction of Cys residue in the primary structure of different human small heat shock proteins in a position homologous to Cys137 of human HspB1 will be useful for investigation of the role of the  $\beta$ 7 strand of different human sHsp in their intersubunit interaction. This paper deals with investigation of the structure and properties of the so-called Cys-mutants of  $\alpha$ B-crystallin, HspB6 and HspB8 containing the single Cys in position homologous to that of human HspB1, and utilization of these Cys-mutants for investigation of intersubunit contacts in homooligomers of different human sHsp.

## Materials and methods

### Proteins

Recombinant wild-type untagged human HspB6, HspB8 and HspB1 were expressed and purified as described earlier (Kasakov et al. 2007; Bukach et al. 2003). The full-length cDNA of  $\alpha$ B-crystallin was amplified from Marathon-Ready Brain cDNA (Clontech) using the following forward GAGATATACAT ATGGACATCGCCATCCACCACC and reverse ATTGCTCGAGCTATTTCTTGGGGC TGCGGT GACAG primers containing *Nde*I and *Xho*I restriction sites (underlined) and *Pfx* Platinum DNA polymerase (Invitrogen). The product thus obtained was treated with *Nde*I and *Xho*I restrictases and ligated into plasmid vector pET21b (Novagen) treated with the same restrictases.

The single-point mutations E117C of  $\alpha$ B-crystallin (HspB5) was obtained by the megaprimer method (Sarkar and Sommer 1990) using E117C CTCCAGGTCCTTCCA CAGGAAATAC and T7 terminator primers.

The double mutant of HspB6 C46S/E116C was obtained by the same approach by subsequent mutation of the wild-type

protein and using E116C GCGCGC TGCTTCCACCGTCG, C46S GCTGCGCTCTCACC CACCACGCTC, T7 promoter and T7 terminator primers.

The mutant of HspB8 containing four-point mutations (C10S/C99S/C195S/N138C) was obtained by PCR by subsequent mutation of the wild-type protein using the following primers GAGATATACATATGGCTGACGGT CAGATGCCCTTCTCCTCTCACTACC (for C10S), GGAAAGTGTCAGTGAATGTGCACAG (for C99S), ATTGCTCGAGTTAGGTTGAGGT GACTTCCTG (for C195S), and CTTTGTGAAGCACTTAGAAACAATG (for N138C). In all cases, the presence of mutation and integrity of sHsp coding sequence was confirmed by DNA sequencing.

The untagged wild-type sHsp and their Cys-mutants were expressed in *E. coli* BL21(DE3). The procedure of recombinant protein isolation consists of ammonium sulfate fractionation, followed by ion-exchange chromatography on High Trap Q (Amersham-Pharmacia; for HspB6 and  $\alpha$ B-crystallin) or hydrophobic chromatography on High Trap Phenyl Sepharose column (for HspB8). On the final stage of purification, HspB6 was subjected to hydrophobic chromatography on High Trap Phenyl Sepharose, whereas  $\alpha$ B-crystallin and HspB8 were subjected to size-exclusion chromatography on Superdex 200 column. Afterwards, all proteins were concentrated, dialyzed against buffer B (20 mM Tris-acetate pH 7.6, 10 mM NaCl, 0.1 mM EDTA, 0.1 mM PMSF and 1 mM DTT), and stored frozen. The protein concentration was determined spectrophotometrically using  $A_{280\text{ nm}}^{0.1\%}$  equal to 0.582 for HspB6 (Swiss-Prot O14558), 0.693 for  $\alpha$ B-crystallin (Swiss-Prot P02489), 1.225 for HspB8 (Swiss-Prot Q9UJY1), and 1.775 for HspB1 (Swiss-Prot P04792).

#### Preparation of reduced and oxidized samples of sHsp

Reduced proteins were obtained by incubation of sHsp (about 1 mg/ml) at 37°C for 30 min in buffer B (20 mM Tris-acetate pH 7.6, 10 mM NaCl, 0.1 mM EDTA, 0.1 mM PMSF) containing 15 mM DTT. Preliminary experiments indicate that this treatment results in complete reduction of all Cys residues. Thus, obtained samples of reduced proteins were either used directly or subjected to different treatments. Oxidation and formation of disulfide bonds was achieved by overnight dialyzes against 50 mM Tris-HCl, pH 7.4, containing 50 mM KCl, 1 mM  $\text{MgCl}_2$ , 0.1 mM PMSF that was performed either at 25 or 37°C. Under these conditions, over 80% of Cys-mutants were crosslinked by disulfide bonds. The protein composition of the samples obtained was determined by SDS-gel electrophoresis performed either on a 15% polyacrylamide gel (Laemmli 1970) or on a 10–20% gradient polyacrylamide gel (Walker 2002).

#### CD spectroscopy

The secondary structure of reduced and oxidized sHsp was analyzed by means of far-UV CD spectroscopy. The samples of reduced proteins were dialyzed overnight at 4°C against 50 mM  $\text{KH}_2\text{PO}_4$ , pH 7.5, 150 mM NaCl, 2 mM DTT. After centrifugation (12,000 $\times$ g, 15 min) the supernatant was used for CD spectroscopy. Oxidized sHsp were prepared by overnight dialyzes of previously reduced proteins against 10 mM Tris-HCl, pH 7.4 containing 50 mM KCl, 2 mM  $\text{MgCl}_2$ , 0.1 mM PMSF at 37°C. The samples thus obtained were subjected to centrifugation (12,000 $\times$ g, 15 min) before spectroscopic measurements. Far-UV CD spectra in the range of 195–260 nm were recorded at 25°C on a Chirascan Circular Dichroism Spectrometer (Applied Photophysics) in cells with optical length of 0.2 mm. The data presented are the average of triplicate measurements with base-line correction using dialyzing buffer. The method of Sreerama and Woody (2000) was used for estimation of the secondary structure of different sHsp.

#### Fluorescence spectroscopy

For measurement of intrinsic Trp fluorescence, the samples of reduced and oxidized sHsp were diluted with buffer B (20 mM Tris-acetate, pH 7.6, 10 mM NaCl, 0.1 mM EDTA, 0.1 mM PMSF) either in the absence or in the presence of 2 mM DTT so that the final protein concentration was equal to 0.06–0.08 mg/ml. The fluorescence was excited at 295 nm (slit width 5 nm) and recorded in the range of 300–400 nm (slit width 5 nm) on a Varian™ CaryEclipse spectrofluorometer at 25°C. Bis-ANS was used for analyzing hydrophobic properties of different samples of sHsp. The sample containing sHsp (0.7–1.0  $\mu\text{M}$  per sHsp monomer) in buffer F (50 mM  $\text{KH}_2\text{PO}_4$ , pH 7.5, 150 mM NaCl, either in the absence or in the presence of 2 mM DTT) was titrated with bis-ANS up to the final concentration 8–9  $\mu\text{M}$ . The fluorescence was excited at 385 nm (slit width 5 nm) and recorded at 495 nm (slit width 5 nm) on a Varian™ CaryEclipse spectrofluorometer at 25°C.

#### Size-exclusion chromatography

Reduced or oxidized samples of sHsp were subjected to size-exclusion chromatography performed on Superdex 75 HR 10/30 or Superdex 200 HR 10/30 columns equilibrated with buffer B (20 mM Tris-acetate pH 7.6, 10 mM NaCl, 0.1 mM EDTA, 0.1 mM PMSF) containing 150 mM NaCl in the absence or in the presence of 15 mM  $\beta$ -mercaptoethanol (ME). The sample (150  $\mu\text{l}$ ) loaded on the column contained different quantities (10–170  $\mu\text{g}$ ) of analyzed proteins. The column was developed at the flow

rate 0.5 ml/min and calibrated with the following protein markers with Stokes radii and molecular masses indicated in parenthesis: thyroglobulin (85 Å, 669 kDa), ferritin (61 Å, 440 kDa), catalase (52 Å, 240 kDa), rabbit skeletal muscle glyceraldehyde-3-phosphate dehydrogenase (42 Å, 144 kDa), bovine serum albumin (35 Å, 68 kDa), ovalbumin (26.8 Å, 43 kDa), chymotrypsin (22.54 Å, 25 kDa), and ribonuclease (17.7 Å, 13.7 kDa).

#### Chaperone-like activity assay

The chaperone-like activity of sHsp was determined by using bovine insulin (Sigma) and bovine liver rhodanese (Fluka) as model protein substrates. In the case of insulin the incubation mixture contained 120 µl of phosphate buffer (100 mM KH<sub>2</sub>PO<sub>4</sub>, 100 mM NaCl, pH 9.0), 100 µl of buffer B (20 mM Tris-acetate, pH 7.6, 10 mM NaCl, 0.1 mM EDTA, 0.1 mM PMSF), variable quantities of sHsp solution and 10 µl of insulin (4–6 mg/ml dissolved in 2.5% acetic acid). The final pH of the incubation mixture was 7.6, the final concentration of insulin was equal to 0.2 mg/ml and the weight ratio sHsp/insulin was equal to 0, 1/4, 1/2, or 1/1. The samples were incubated for 2 min at 37°C and reaction was started by addition of 20 µl of 300 mM solution of DTT up to the final concentration 24 mM.

In the case of rhodanese, the incubation mixture contained 150 µl of 100 mM phosphate buffer (pH 7.7) and 150 µl of buffer B (20 mM Tris-acetate, pH 7.6, 10 mM NaCl, 0.1 mM EDTA, 0.1 mM PMSF). The concentration of rhodanese in the incubation mixture was constant and equal to 0.2 mg/ml, whereas the concentration of sHsp varied from 0 up to 0.2 mg/ml, so that the weight ration sHsp/rhodanese was equal to 0, 1/4, 1/2, or 1/1. The experiments were performed either in the absence of DTT (for oxidized samples of sHsp) or in the presence of 1.5 mM of DTT (for reduced samples of sHsp). The samples were incubated for 10 min at 25°C and afterwards transferred to the optical cells heated up to 44°C.

Reduction-induced aggregation of insulin or heat-induced aggregation of rhodanese was monitored for 40–60 min by recording optical density at 360 nm on a Ultraspec 3100 Pro spectrophotometer.

## Results

#### Design and purification of Cys-mutants of human small heat shock proteins

Mouse Hsp25 containing the single Cys141 located in the β7 strand is easily oxidized with formation of disulfide

crosslinked dimers (Zavialov et al. 1998a, b). We supposed that the β7 strand is involved in the subunit interaction of different human sHsp. In order to check this suggestion, we introduced Cys residues into the structure of human αB-crystallin, HspB6 and HspB8 in a position homologous to that of Cys141 of mouse Hsp25 (or Cys137 of human HspB1). The human wild-type αB-crystallin does not contain intrinsic Cys residues and the multiple alignment of human sHsp (Kasakov et al. 2007; Michiel et al. 2009; Bagneris et al. 2009) indicates that Glu117 of αB-crystallin is in a position homologous to that of Cys137 of HspB1. Therefore, we introduced the single-mutation E117C into the structure of human αB-crystallin (Fig. 1a). HspB6 contains the single Cys46 in the variable N-terminal end and Glu116 in a position homologous to Cys137 of HspB1 (Kasakov et al. 2007; Michiel et al. 2009; Bagneris et al. 2009). To exclude the effect of Cys46 of HspB6 on the subunit interaction we replaced this residue by Ser and mutated Glu116 to Cys, thus obtaining the so-called Cys-mutant (C46S/E116C) of HspB6 (Fig. 1a). HspB8 contains three Cys residues located in the variable N-terminal (C10) and C-terminal (C195) ends and in the α-crystallin domain (C99). All these residues were replaced by Ser and Asn138 located in a position homologous to Cys137 of HspB1 was

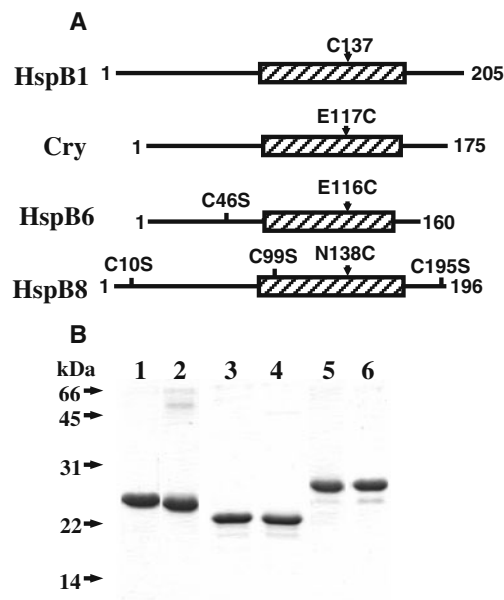


**Fig. 1** **a** The scheme of the structure of HspB1, αB-crystallin (*Cry*), HspB6 and HspB8 with location of mutated Cys residues and indication of single Cys inserted in the β7 strand in position homologous to Cys137 of Hsp27. Crystallin domain is shown as a hatched rectangle and the total number of amino acid residue is indicated for each sHsp. **b** SDS-electrophoresis of the wild-type αB-crystallin (1) and its Cys-mutant (E117C) (2), of the wild-type HspB6 (3) and its Cys-mutant (C46S/E116C) (4), of the wild-type HspB8 (5) and its Cys-mutant (C10S/C99S/C195S/N138C) (6). The positions of molecular mass standards (in kDa) are indicated by arrows

replaced by Cys. Thus, the so-called Cys-mutant of HspB8 contained four-point mutations C10S/C99S/C195S/N138C (Fig. 1a). By using earlier described methods (Kasakov et al. 2007; Bukach et al. 2003) and procedure described in the “Materials and methods” section we purified the wild-type human  $\alpha$ B-crystallin, HspB6 and HspB8, and their Cys-mutants (Fig. 1b) and found that the mutations introduced do not affect the electrophoretic mobility of these proteins in SDS-gel electrophoresis. Before investigation of protein–protein interaction, we compared the physico-chemical properties of the wild-type proteins and their Cys-mutants.

#### Spectroscopic investigations of the wild-type proteins and their Cys-mutants

Far-UV CD spectroscopy was used for investigation of the secondary structure of human sHsp. The CD spectra of the wild-type  $\alpha$ B-crystallin and its Cys-mutant have a broad negative maximum between 208 and 215 nm (Fig. 2a) and the amplitude of this maximum was practically identical for the wild-type protein and its

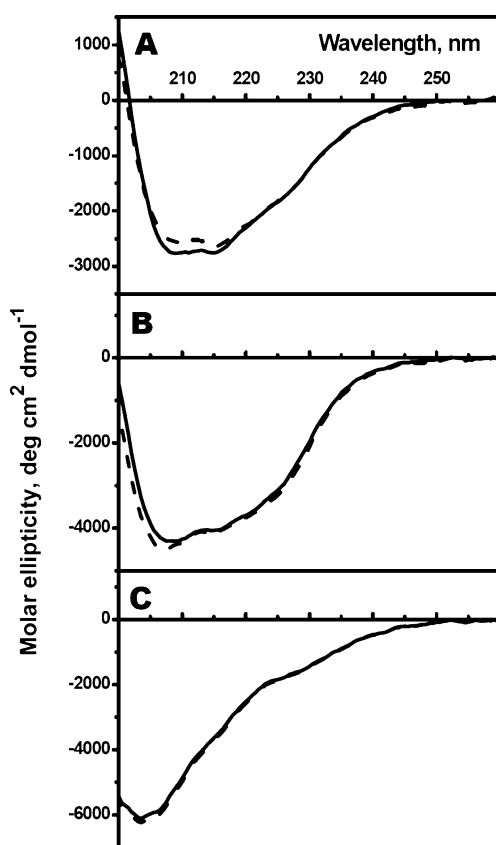


**Fig. 2** The far-UV CD spectra of the wild type (solid lines) or Cys-mutants (dashed lines) of  $\alpha$ B-crystallin (a), HspB6 (b), and HspB8 (c). The data presented are the average of triplicate measurements with base-line correction

Cys-mutant and close to the values reported in the literature (Murugesan et al. 2008). The negative maximum of HspB6 far-UV CD spectrum is shifted to 208 nm (Fig. 2b). The shape and amplitude of the far-UV CD spectrum of the wild-type HspB6 and its Cys-mutant were practically indistinguishable thus indicating that the double mutation (C46S/E116C) does not affect the secondary structure. The CD spectrum of Hsp22 was characterized by a negative maximum at about 205 nm and the amplitude and position of this maximum were again indistinguishable for the wild-type protein and its Cys-mutant (Fig. 2c). This means that the fourfold mutation (C10S/C99S/C195S/N138C) does not affect the secondary structure of HspB8. Estimation of the secondary structure based on the data of far-UV CD spectroscopy indicates that the analyzed human sHsp and their Cys-mutants have similar or identical structure and contain very small quantities of  $\alpha$ -helices and is enriched by  $\beta$ -strands (35–37%), turns (22–23%), and unordered structure (33–35%; Online Resource 1).

The method of intrinsic fluorescence was used for analyzing environment and tertiary structure around Trp residues of human sHsp and their Cys-mutants. The fluorescence spectra of all proteins analyzed were characterized by a broad maximum at about 345–346 nm and mutations practically do not affect the amplitude or position of fluorescence maximum (Fig. 3). The data presented mean that the tertiary structure of Cys-mutants was similar to that of the wild-type proteins and that in all cases the largest portion of Trp residues was located on the protein surface (Permyakov 1993).

Finally, the hydrophobic properties of human sHsp and their Cys-mutants were probed by using bis-ANS. The fluorescence of free bis-ANS is very low and is significantly increased after binding to hydrophobic sites of proteins. Titration of  $\alpha$ B-crystallin or its Cys-mutants with bis-ANS was accompanied by an increase of fluorescence that tends to saturate at high bis-ANS concentrations (Online Resource 2). Since we have not observed any difference in titration curve of the wild-type  $\alpha$ B-crystallin and its Cys-mutants, we may conclude that mutation E117C does not affect the hydrophobic properties of  $\alpha$ B-crystallin. Titration of the wild-type HspB6 and HspB8 and of their Cys-mutants with bis-ANS in a wide concentration range was accompanied by a linear increase of fluorescence (data not shown). This correlates with our earlier published data and indicates the presence of a large number of low-affinity binding sites on the surface of these proteins (Kasakov et al. 2007; Kim et al. 2006). In all cases, the difference of the titration curves of the wild-type proteins and their Cys-mutants was minimal thus indicating that mutations introduced do not dramatically affect the hydrophobic properties of sHsp.

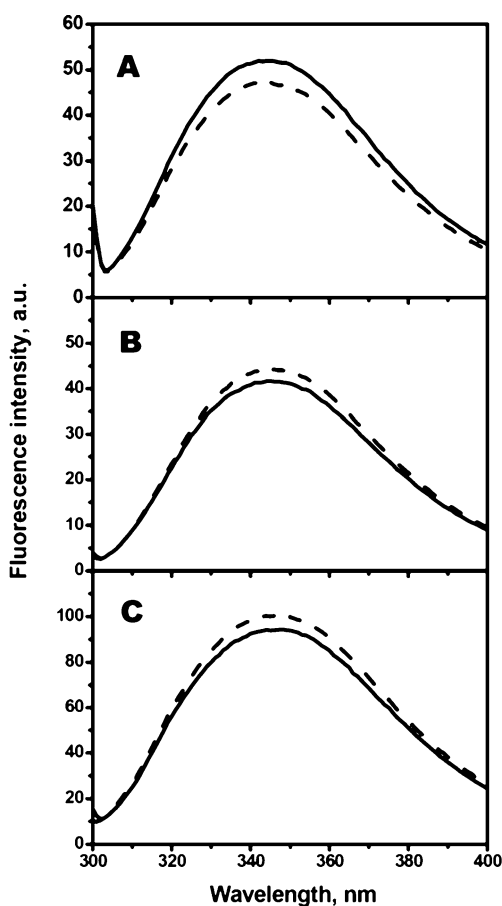


**Fig. 3** Intrinsic Trp fluorescence of the wild type (solid lines) or Cys-mutants (dashed lines) of  $\alpha$ B-crystallin (a), HspB6 (b), and HspB8 (c). The fluorescence was excited at 295 nm and recorded in the range 300–400 nm. The data presented are the average of triplicate measurements with at least two different protein samples

#### Quaternary structure of sHsp and their Cys-mutants

Size-exclusion chromatography was used for investigation of quaternary structure of sHsp. Independent of the quantity of protein loaded on the column,  $\alpha$ B-crystallin and its Cys-mutant were eluted as a symmetric peak close to the exclusion volume of Superdex 200 column (Fig. 4a). The apparent molecular mass of the wild-type  $\alpha$ B-crystallin was close to 540 kDa and that of Cys-mutant close to 570 kDa.

As reported earlier (Bukach et al. 2003), the wild-type HspB6 was eluted as a single symmetric peak with an apparent molecular mass of 53–57 kDa probably corresponding to dimer. The elution volume was independent of the quantity of protein loaded on the column (Fig. 4b) and the chromatographic properties of Cys-mutant of HspB6 were indistinguishable from those of the wild-type protein.

In the course of the size-exclusion chromatography, HspB8 seems to be present in the form of an equilibrium mixture of monomers and dimers (Kasakov et al. 2007;

Kim et al. 2006). Therefore, elution volume depends on the quantity of protein loaded on the column (Fig. 4c). The chromatographic properties of Cys-mutant were similar to those of the wild-type HspB8, however at all concentrations used the elution volume of Cys-mutant was slightly smaller than that of the wild-type protein thus indicating that mutations C10S/C99S/C195S/N138C only slightly affect the size or the shape of Hsp22.

#### Chaperone-like activity of human sHsp

One of the main functions of sHsp is their ability to prevent or to retard aggregation of partially denatured proteins (Haslbeck et al. 2005; Vos et al. 2008; Mchaourab et al. 2009). Therefore, we compared the chaperone-like activity of the wild-type proteins and their Cys-mutants using

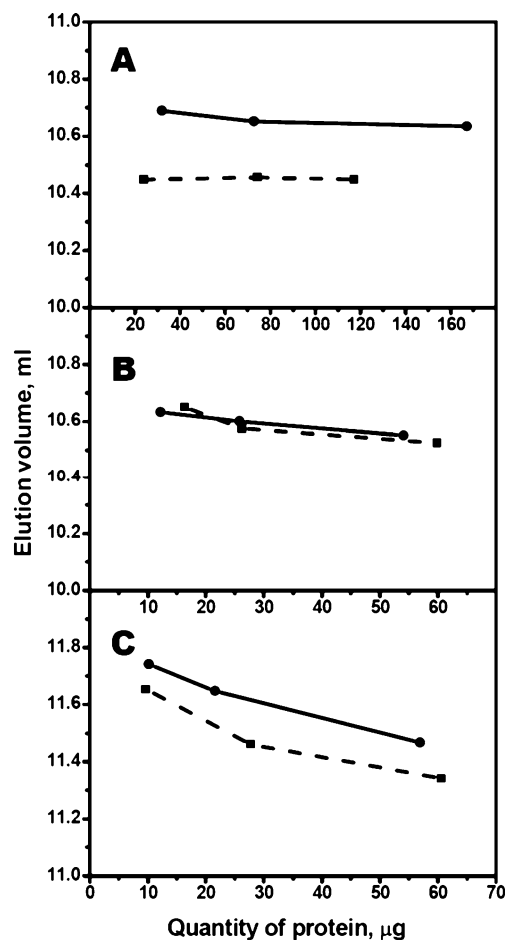


**Fig. 4** Dependence of elution volume on the quantity of  $\alpha$ B-crystallin (a), HspB6 (b), and HspB8 (c) loaded on the Superdex column. The size-exclusion chromatography of  $\alpha$ B-crystallin (a) was performed on Superdex 200 HR10/30 column and the chromatography of HspB6 (b), and HspB8 (c) was performed on Superdex 75 HR 10/30 column. Each experiment was repeated at least twice. Solid lines correspond to the wild-type proteins, and the dashed lines correspond to their Cys-mutants

rhodanese and insulin as model substrates. Addition of  $\alpha$ B-crystallin or its Cys-mutant at the weight ratio sHsp/rhodanese equal to 1/2 completely prevented heat-induced aggregation of rhodanese (Fig. 5a). Similar results were obtained if the weight ratio rhodanese/ $\alpha$ B-crystallin was equal to 1/4 or 1/1 (data not shown). Reduction-induced aggregation of insulin was also retarded or completely prevented by addition of  $\alpha$ B-crystallin and the efficiency of Cys-mutant was identical to that of the wild-type protein (Online Resource 3).

At the weight ratio sHsp/rhodanese equal to 1/2 the wild-type HspB6 inhibited aggregation of rhodanese, and the chaperone-like activity of its Cys-mutant was similar to that of the wild-type protein (Fig. 5b). Similar results were obtained at the weight ratio HspB6/rhodanese equal to 1/1 (data not shown). Both the wild-type HspB6 and its Cys-

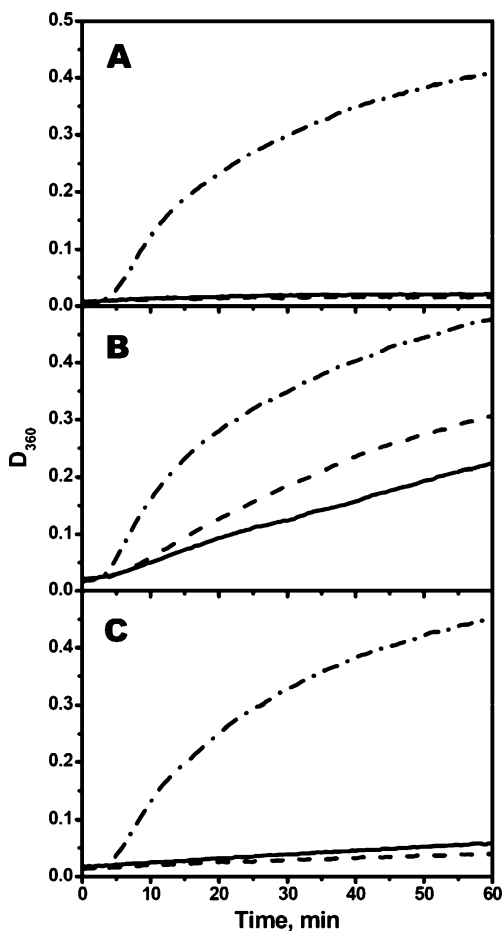


**Fig. 5** Chaperone-like activity of  $\alpha$ B-crystallin (a), HspB6 (b), and HspB8 (c) measured by their ability to affect heat-induced aggregation of rhodanese. Aggregation of rhodanese was induced by heating up to 44°C and was recorded by increase of the optical density at 360 nm. Aggregation of rhodanese was measured in the absence of sHsp (dash-dotted lines) or in the presence of the wild-type sHsp (solid lines) or their Cys-mutants (dashed lines). The weight ratio sHsp/rhodanese was equal to 1/2

mutant inhibited reduction-induced aggregation of insulin; however, the chaperone-like activity of the wild-type protein was higher than that of Cys-mutant (Online Resource 3). We suppose that decreased chaperone-like activity of Cys-mutant of HspB6 with insulin is predominantly induced by mutation C46S in the N-terminal part of the protein. The data of literature indicate that the peptides containing residues 11–18 and 33–40 of  $\alpha$ B-crystallin (which are homologous to peptides containing residues 13–23 and 38–46 of HspB6) are directly involved in insulin binding (Ghosh et al. 2007). The last site is located close to Cys46 of HspB6 and therefore mutation C46S might affect the chaperone-like activity of Cys-mutant of HspB6 with insulin as a model protein substrate.

The wild-type HspB8 and its Cys-mutant had comparable chaperone-like activity if rhodanese (Fig. 5c) or insulin (Online Resource 3) were used as model protein substrates. Similar results were obtained at different weight ratios of HspB8/protein substrate thus indicating that the chaperone-like activity of Cys-mutant of Hsp22 is comparable with that of the wild-type protein.

Summing up, we may conclude that the secondary, tertiary and quaternary structure of Cys-mutants as well as their chaperone-like activity is practically indistinguishable from those of the wild-type proteins and this makes possible utilization of Cys-mutants for further investigation of intersubunit contacts in sHsp oligomers.

#### Formation of disulfide bonds in the wild-type sHsp and their Cys-mutants

The data of Zavialov et al. (1998a, b) indicate that incubation under non-reducing conditions of mouse Hsp25 containing a single Cys141 is accompanied by formation of disulfide crosslinked dimers. We supposed that human HspB1 containing the single Cys137 in a position homologous to that of mouse Hsp25 as well as the other human sHsp containing the single Cys in similar positions would also be able to form oxidized dimers.

The wild-type  $\alpha$ B-crystallin does not contain Cys residues and therefore dialysis under non-reducing condition does not lead to formation of dimers. At the same time, the Cys-mutant of  $\alpha$ B-crystallin effectively forms disulfide crosslinked dimers (Fig. 6a).

As reported earlier, oxidation of the wild-type HspB6 containing the single Cys46, is accompanied by accumulation of crosslinked dimers with an apparent molecular mass of about 43 kDa (Bukach et al. 2003). The Cys-mutant of HspB6 containing the single Cys116 was easily oxidized with the formation of a crosslinked dimers with an apparent molecular mass 43 kDa (Fig. 6b). Comparing the intensity of the band of remaining uncrosslinked monomer in the case of the wild-type HspB6 (Fig. 6b, lane 2) and in the

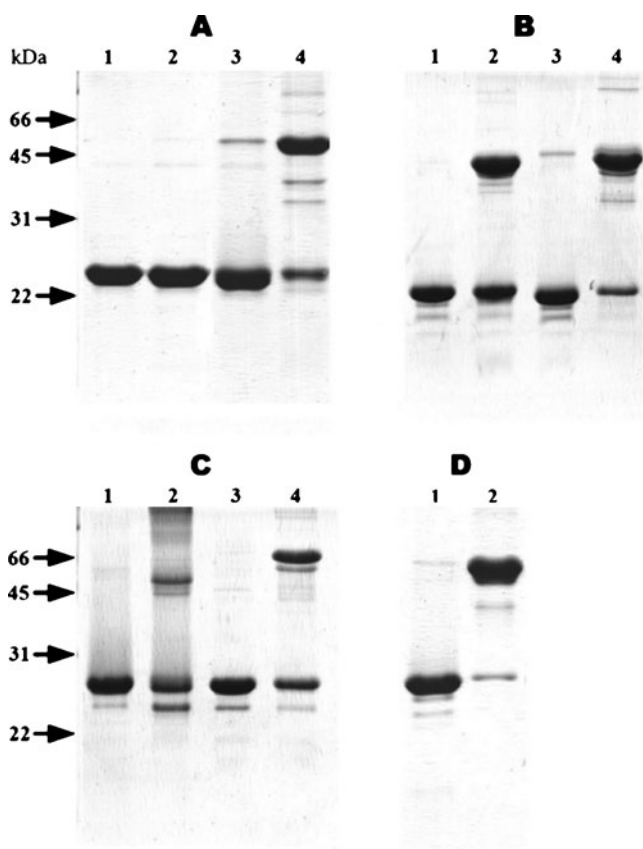


**Fig. 6** Disulfide crosslinking of  $\alpha$ B-crystallin (a), HspB6 (b), HspB8 (c) and HspB1 (d). The wild-type proteins (lanes 1 and 2) or their Cys-mutants (lanes 3 and 4) were analyzed by non-reducing SDS-gel electrophoresis before (lanes 1 and 3) or after (lanes 2 and 4) overnight dialysis under non-reducing conditions at 25°C. The positions of molecular mass standards (in kilodaltons) are indicated by arrows

case of the Cys-mutant of HspB6 (Fig. 6b, lane 4) we may conclude that the probability of crosslinking of Cys-mutant was higher than that of the wild-type protein.

Under oxidation conditions, the wild-type HspB8 containing three Cys residues (Cys10, Cys99, and Cys195) is chaotically crosslinked with formation of both intra- and intersubunits disulfide bonds and accumulation of dimers with an apparent molecular mass of 43–45 kDa as well as unordered crosslinked oligomers of high molecular mass that do not enter the gel (Kim et al. 2004; Fig. 6c, lane 2). Oxidation of Cys-mutant of HspB8 containing the single Cys138 leads to formation of only dimers with an apparent molecular mass 56–58 kDa (Fig. 6c, lane 4).

Under conditions used, the efficiency of crosslinking of HspB1 (Fig. 6d) was comparable with that of Cys-mutants of the other sHsp (Fig. 6a–c). We found that efficiency of crosslinking is temperature-dependent and dialysis under non-reducing conditions at 37°C was accompanied by crosslinking of more than 80% of sHsp monomers (Online Resource 4). Thus, we may conclude that Cys located in the

$\beta$ 7 strand is close to intersubunits and can be used for formation of disulfide crosslinked dimers of all analyzed human sHsp.

#### Spectroscopic investigation of oxidized Cys-mutants of human sHsp

Finding optimal conditions of crosslinking when more than 80% of the proteins were presented in the form of oxidized dimers we were able to compare the structure and properties of oxidized and reduced Cys-mutants of sHsp. The data of far-UV CD spectroscopy show that oxidation of Cys-mutants of all sHsp was accompanied by a slight increase of negative ellipticity at 205–220 nm (Fig. 7). Estimation of the secondary structure indicates that these changes might reflect a small (less than 2–3%) decrease in the quantity of  $\beta$ -strand and a corresponding 2–3% increase in the quantity of turns and/or unordered structure. In any case, formation of disulfide bond was accompanied by less than a 10% change in the overall content of both  $\beta$ -strand and unordered structures.

Analyzing intrinsic Trp fluorescence, we found that oxidation does not affect position of fluorescence maximum

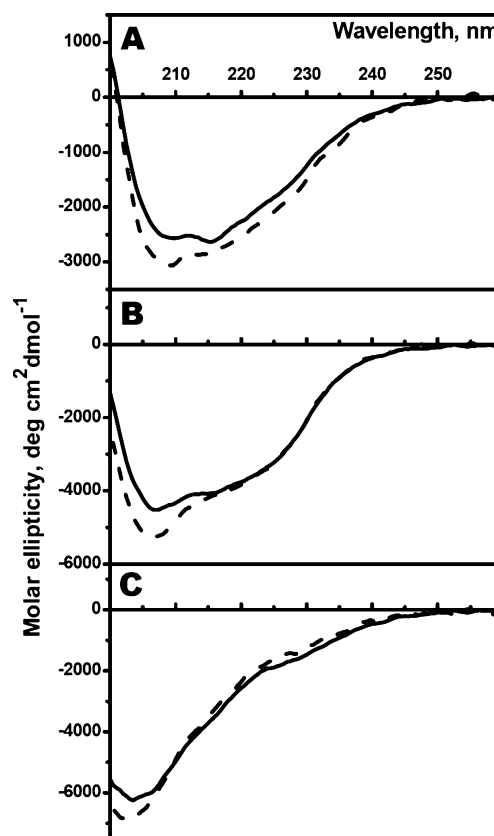


**Fig. 7** Far-UV CD spectra of reduced (solid line) and oxidized (dashed line) Cys-mutants of  $\alpha$ B-crystallin (a), HspB6 (b), and HspB8 (c). The data presented are the average of triplicate measurements with base-line correction



of all Cys-mutants (Online Resource 5). This means that oxidation of Cys-mutants does not significantly affect environment or mobility of Trp residues of all proteins analyzed. The data presented indicate that crosslinking of the neighboring subunits of sHsp by the disulfide bond does not induce dramatic alterations both in the secondary and in the tertiary structure of these proteins.

#### Quaternary structure of oxidized Cys-mutants of human sHsp

Size-exclusion chromatography on Superdex 200HR10/30 column was used for analyzing effect of disulfide crosslinking on the quaternary structure of Cys-mutants. Both reduced and oxidized Cys-mutants of  $\alpha$ B-crystallin were eluted as symmetrical peaks with apparent molecular mass of 550–570 kDa, i.e., with molecular mass comparable with that of the wild-type  $\alpha$ B-crystallin (540–560 kDa; Fig. 8a). This means that formation of disulfide crosslinked dimers does not affect the oligomeric structure of  $\alpha$ B-crystallin that independent on crosslinking forms high-molecular-mass oligomers of similar size.

Both oxidized and reduced Cys-mutants of HspB6 were eluted as a single peaks with apparent molecular mass of about 53–57 kDa, that was indistinguishable from the wild-type HspB6 (Fig. 8b). These data mean that under conditions used both the wild-type HspB6 and its reduced or oxidized Cys-mutants predominantly form stable dimers that are not dissociated in the course of size-exclusion chromatography and that formation of disulfide bond does not affect the size or the shape of HspB6 dimers.

As already mentioned, the wild-type HspB8 and its reduced Cys-mutant were eluted on the size-exclusion chromatography as a peak with an apparent molecular mass of 30–38 kDa and position of this peak was dependent on the quantity of protein loaded on the column (Fig. 4c; Kasakov et al. 2007; Kim et al. 2006). This might indicate that under conditions of chromatography, HspB8 is presented in the form of an equilibrium mixture of monomer and dimer and this equilibrium depends on the protein concentration. Destabilization of intersubunit contacts of HspB8 can be due to at least two factors. Firstly, this protein is lacking conservative hydrophobic stretch I–X–I/V in the variable C-terminal tail, and secondly the multiple alignment (Michiel et al. 2009; Bagneris et al. 2009) indicates that the primary structure of HspB8 makes impossible formation of  $\beta 2$  strand of  $\alpha$ -crystallin domain. Both the hydrophobic stretch in the C-terminal tail and  $\beta 2$  strand might participate in formation of intersubunit contacts (Stamler et al. 2005; Bagneris et al. 2009). The absence of both these elements destabilizes intersubunit contacts of HspB8 and provokes dissociation of HspB8 dimers. Probably, therefore, reduced Cys-mutant of HspB8

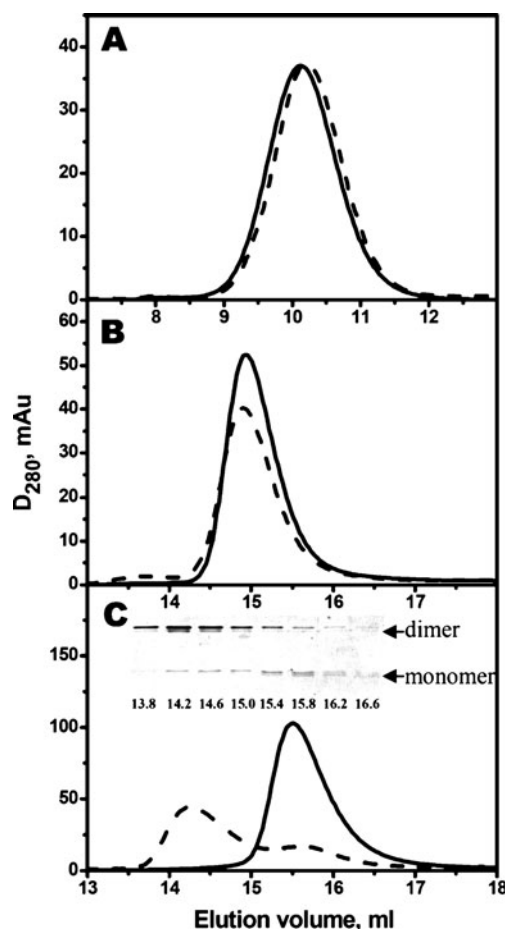


**Fig. 8** Size-exclusion chromatography of reduced (*solid line*) and oxidized (*dashed line*) Cys-mutants of  $\alpha$ B-crystallin (**a**), HspB6 (**b**), and HspB8 (**c**) on Superdex 200 HR10/30 column. Representative elution profiles of at least three different experiments are presented. *Insert* in **c** represents the protein composition (determined by non-reduced SDS-gel electrophoresis) of the fractions with elution volumes indicated under each lane. Positions of monomer and dimer of HspB8 are indicated by *arrows*

was eluted as a peak with an apparent molecular mass of 30–38 kDa corresponding to equilibrium mixture of monomers and dimers (Fig. 8c). At the same time, the oxidized Cys-mutant of HspB8 was eluted as two poorly separated peaks (Fig. 8c). The first peak with apparent molecular mass 66–70 kDa (elution volume about 14.2 ml) contained according to the data of SDS-electrophoresis (performed under non-reducing conditions) predominantly disulfide crosslinked dimers of HspB8 (Fig. 8c), whereas the second peak with apparent molecular mass 33–36 kDa (elution volume 15.8 ml) predominantly contained monomers of HspB8. Cys-mutant of HspB8 is easily oxidized and this explains the presence of small quantity of cross-linked dimers detected in the second peak (elution volume 15.8 ml) that probably were formed already after the size-exclusion chromatography. The data presented mean that Cys located in the  $\beta 7$  strand is close to intersubunit

contacts and formation of disulfide bond stabilizes the structure of HspB8 dimers.

#### Chaperone-like activity of oxidized Cys-mutants of sHsp

We also tried to compare the chaperone-like activity of reduced and oxidized Cys-mutants of sHsp. Since aggregation of insulin is induced by reduction of its disulfide bonds, we were unable to use this model substrate for comparison of chaperone-like activity of reduced and oxidized mutants. Therefore, the chaperone-like activity of Cys-mutant was determined by their ability to inhibit thermal-induced aggregation of rhodanese. However, even in this case, the kinetics of rhodanese aggregation is dependent on the presence of DTT in the incubation mixture and therefore in all experiments performed in the absence of DTT (Fig. 9) the increase of the optical density

was less than in the same experiments performed in the presence of DTT (Fig. 5). The data of Fig. 9 indicate that the chaperone-like activity is independent on whether Cys-mutants of sHsp were in reduced (solid lines) or oxidized (dashed lines) state. It is worthwhile to mention that these experiments were performed at elevated temperature (44°C) and in the absence of DTT, i.e., under conditions favoring oxidation of Cys residues. Therefore, at the end of incubation, a rather large portion of initially reduced Cys-mutants of sHsp became oxidized and formed disulfide crosslinked dimers (data not shown). However, gradual accumulation of disulfide crosslinked dimers did not affect the kinetics of rhodanese aggregation (Fig. 9), thus indicating that formation of dimers crosslinked by disulfide bond does not dramatically affect the chaperone-like activity of sHsp.

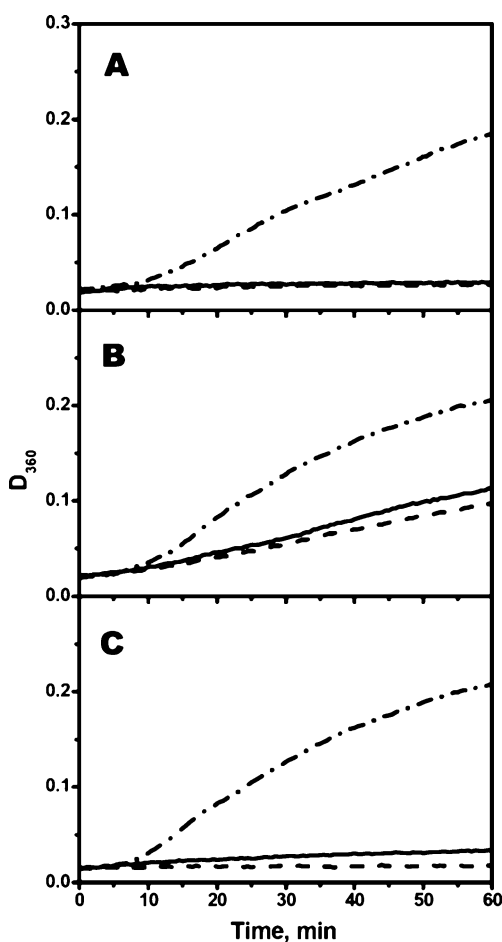


**Fig. 9** Chaperone-like activity of reduced and oxidized Cys-mutants of  $\alpha$ B-crystallin (a), HspB6 (b), and HspB8 (c) measured by their ability to inhibit heat-induced aggregation of rhodanese. Aggregation of rhodanese was measured in the absence of sHsp (dash-dotted lines) or in the presence of reduced (solid lines) or oxidized (dashed lines) Cys-mutants of different sHsp. The weight ratio sHsp/rhodanese was equal to 1/2

#### Discussion

Up until now, all attempts to crystallize full-length human sHsp were unsuccessful and therefore detailed three-dimensional structures of these proteins remains unknown. Intersubunit contacts were analyzed either by indirect methods or using different fragments of sHsp and predominantly for  $\alpha$ B-crystallin and to a smaller extent for HspB1 (Berengian et al. 1999; Ghosh and Clark 2005; Jehle et al. 2009; Feil et al. 2001), whereas all other human sHsp remain poorly investigated. We tried to analyze the intersubunit contacts of three human sHsp by inserting the single Cys residue in a position homologous to that of Cys137 of human HspB1. This site was chosen since the data of literature (Zavialov et al. 1998a, b) indicate that the mouse Hsp25 is easily oxidized with the formation of dimers crosslinked by disulfide bond formed by two Cys141 residues belonging to the neighboring subunits. Human HspB1 contains the single Cys137 in position homologous to Cys141 of murine Hsp25. These Cys residues are solvent-exposed and are easily accessible for low-molecular-mass thiols (Berengian et al. 1999; Zavialov et al. 1998b; Eaton et al. 2002). In addition Glu113 of  $\alpha$ A-crystallin and Glu117 of  $\alpha$ B-crystallin, i.e., residues homologous to Cys137 of HspB1, were postulated to be located on the solvent-exposed surface of  $\beta$ -strand and these residues seem to be close to each other in  $\alpha$ A- or  $\alpha$ B-crystallin dimers (Berengian et al. 1997, 1999).

Utilization of Cys-mutants (i.e., mutants containing the single Cys in position homologous to Cys137 of HspB1) for analyzing intersubunit contacts of different sHsp will be useful only if mutations introduced do not perturb the structure and properties of the proteins investigated. By using far-UV CD and fluorescence spectroscopy we found that the secondary and tertiary structure of Cys-mutants was

not significantly different from that of the wild-type proteins (Figs. 2 and 3). Introduction of the single Cys residues into the  $\beta 7$  strand and replacement of intrinsic Cys residues by Ser had no significant effect on the hydrophobic properties measured by bis-ANS binding or on the quaternary structure of human sHsp (Online Resource 2 and Fig. 4). If rhodanese was used as a model substrate, the chaperone-like activity of Cys-mutants of all sHsp was similar to that of the wild-type proteins (Fig. 5). Thus, the introduction of Cys in a position homologous to Cys137 of HspB1 per se does not dramatically affect the structure and properties of sHsp. It is worthwhile to mention that mutation of the neighboring residues often leads to significant changes in the structure and properties of sHsp. For instance, mutation R120G results in the change of oligomeric structure, chaperone-like activity, and intersubunit interaction of  $\alpha B$ -crystallin (Kumar et al. 1999; Perng et al. 1999; Simon et al. 2007; Michiel et al. 2009; Bova et al. 1999). Similar effects were observed in the case of HspB8 where mutations K137E and/or K141E were also accompanied by significant changes in the structure and properties (Kasakov et al. 2007; Kim et al. 2006). This difference can be due to the fact that positions occupied by conservative Arg or Lys residues (Arg120 of  $\alpha B$ -crystallin and Lys141 of HspB8) are located inside of the sHsp monomer and are involved in many intra- and intermonomer contacts (Michiel et al. 2009; Berengian et al. 1997, 1999; Simon et al. 2007). This suggestion was very recently confirmed by X-ray investigation of the structure of isolated  $\alpha$ -crystalline domain of  $\alpha B$ -crystallin and HspB6 (Bagneris et al. 2009; Fig. 10). The contacts formed by these positively charged residues control the flexibility and orientation of the  $\beta 7$  strand and thus intersubunit interaction (Michiel et al. 2009). At the same time, Cys located in

a position homologous to Cys137 of HspB1 seem to be located on the monomer surface (Berengian et al. 1997, 1999; Fig. 10) and probably therefore mutation of this position does not dramatically affect the structure and properties of sHsp.

Since introduction of Cys into the  $\beta 7$  strand does not perturb the structure, we were able to utilize Cys-mutants for investigation of intersubunit contacts of different human sHsp. Mild oxidation of all Cys-mutants leads to formation of sHsp dimers crosslinked by disulfide bonds and the efficiency of this process was comparable with that of the wild-type HspB1 (Fig. 6, Online Resource 4). This means that the  $\beta 7$  strand of two neighboring monomer having antiparallel orientation are located close to each other and this makes possible formation of disulfide bond. This conclusion agrees with the data obtained on mutated  $\alpha A$ -crystallin (Berengian et al. 1997) and on the wild-type HspB1 (Berengian et al. 1999), as well as with the data obtained by peptide pin array techniques (Sreelakshmi et al. 2004). Very recently, published results obtained on isolated  $\alpha$ -crystallin domain of  $\alpha B$ -crystallin (Bagneris et al. 2009) also indicate that Glu117 (replaced by Cys in our experiments) of two neighboring subunits of  $\alpha B$ -crystallin are located on the protein surface in close vicinity to each other (Fig. 10). This might indicate that orientation of the  $\beta 7$  in the isolated  $\alpha$ -crystallin domain and in the full size protein is similar. At the same time, it is worthwhile to mention that our results disagree with the data of Ghosh et al. (Ghosh and Clark 2005; Ghosh et al. 2007) who, using peptide pin array, failed to detect involvement of  $\beta 7$  strand in the intersubunit contacts. This probably can be due to the changes in the structure of short peptides corresponding to the  $\beta 7$  strand upon their immobilization on plastic surface.

Formation of disulfide bonds between two monomers has only marginal effect on the secondary and tertiary structure of sHsp (Fig. 7, Online Resource 5). Disulfide crosslinking does not affect the oligomeric structure of  $\alpha B$ -crystallin and HspB6 (Fig. 8a, b) and shifts the equilibrium between monomer and dimer of HspB8 towards formation of dimers (Fig. 8c). In addition, formation of disulfide bond does not induce dramatic changes in the chaperone-like activity of all analyzed sHsp (Fig. 9). It is worthwhile to mention that in vivo oxidative stress results in reversible formation of disulfide crosslinked dimers of mouse Hsp25 and human HspB1 (Zavialov et al. 1998b; Diaz-Latoud et al. 2005) and even under normal conditions small portion of mouse Hsp25 remained in the form of oxidized dimer (Zavialov et al. 1998a). The wild-type HspB1 effectively protected the cells against oxidative stress, whereas C137A mutant, lacking the unique cysteine was almost completely ineffective (Arrigo et al. 2005). All these data indicate that HspB1 can undergo reversible transitions from reduced to oxidized state and that these transitions somehow affect

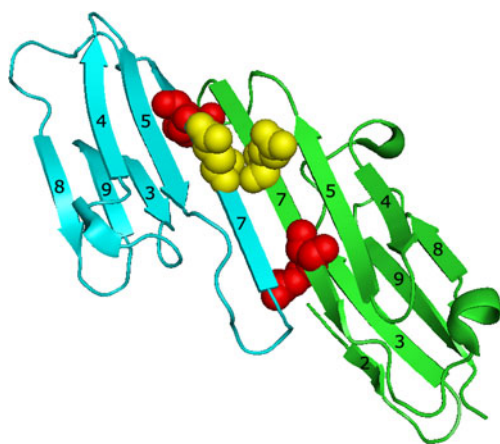


**Fig. 10** Dimer of isolated  $\alpha$ -crystallin domain of  $\alpha B$ -crystallin (Bagneris et al. 2009; PDB code 2wj7). Two monomers are colored *blue* and *green*, Glu117 replaced by Cys in this investigation (*gold*) and conservative Arg120 (*red*) are space-filled. The  $\beta$  strands of each monomer are numbered

resistance of the cell to oxidative stress. We might suppose that our Cys-mutants of different sHsp if expressed in the cell will also be able to control its red-ox state.

Summing up, we may conclude that the structure and properties of Cys-mutants described in this paper are similar to those of the wild-type proteins. Therefore, these Cys-mutants can be successfully used for investigation of the structure and properties of different sHsp. The data obtained mean that the  $\beta 7$  strand is involved in the intersubunit contacts of human  $\alpha B$ -crystallin, HspB1, HspB6, and HspB8. These proteins differ in the length and structure of variable N- and C-terminal ends and in the presence (HspB1, HspB6 and  $\alpha B$ -crystallin) or in the absence (HspB8) of  $\beta 2$  strand in the  $\alpha$ -crystallin domain. Both the hydrophobic stretch in the C-terminal tail and the  $\beta 2$  strand of  $\alpha$ -crystallin domain play important role in the intersubunit interactions (Mchaourab et al. 2009; Stamler et al. 2005; van Monfort et al. 2001). However, despite all differences in the structure, all sHsp analyzed preserve their ability to form intersubunit contacts with participation of  $\beta 7$  strand thus indicating the pivotal role of this strand in monomer–monomer interaction. Formation of disulfide bond between two monomers does not dramatically affect the overall structure of sHsp. We suppose that there are three lines of future investigations that can use Cys-mutants of sHsp. Firstly, the Cys-mutants can be used for investigation of formation of heterooligomeric complexes between different sHsp. Our preliminary data indicate that Cys-mutants readily form disulfide crosslinked heterodimers. Secondly, the Cys-mutants can be used for crystallization of full-length proteins, since introduction of disulfide bond usually stabilize flexible regions of protein structure. Thirdly, expression of Cys-mutants of different sHsp in eukaryotic cells might modulate their resistance to oxidative stress. Cys137 seems to be important for the interaction of HspB1 with cytochrome *c* and for antiapoptotic activity of HspB1 (Bruey et al. 2000). Therefore, we might speculate that expression of Cys-mutants of the other human sHsp will also somehow affect their antiapoptotic activity.

**Acknowledgment** This investigation was supported by the Russian Foundation for Basic Research.

## References

- Arrigo AP, Simon S, Gibert B, Kretz-Remy C, Nivon M, Czekalla A, Guillet D, Moulin M, Diaz-Latoud C, Vicart P (2007) Hsp27 (HspB1) and  $\alpha B$ -crystallin (HspB5) as therapeutic targets. *FEBS Lett* 581:3665–3674
- Arrigo AP, Viot S, Chaufour S, Firdaus W, Kretz-Remy C, Diaz-Latoud C (2005) Hsp27 consolidates intracellular redox homeostasis by uploading glutathione in its reduced form and by decreasing iron intracellular levels. *Antioxid Redox Signal* 7:414–424
- Bagneris C, Bateman OA, Naylor CE, Cronin N, Boelens WC, Keep NH, Slingsby C (2009) Crystal structure of  $\alpha$ -crystallin domain dimers of  $\alpha B$ -crystallin and Hsp20. *J Mol Biol* 392:1242–1252
- Benndorf R, Welsh MJ (2004) Shocking degeneration. *Nat Genet* 36:547–548
- Berengian AR, Bova MP, Mchaourab HS (1997) Structure and function of the conserved domain in  $\alpha A$ -crystallin. Site-directed spin labeling identifies a  $\beta$ -strand located near a subunit interface. *Biochemistry* 36:9951–9957
- Berengian AR, Parfenova M, Mchaourab HS (1999) Site-directed spin labeling study of subunit interactions in the  $\alpha$ -crystallin domain of small heat-shock proteins. *J Biol Chem* 274:6305–6314
- Bova MP, Yaron O, Huang Q, Ding L, Haley DA, Stewart PL, Horwitz J (1999) Mutation R120G in  $\alpha B$ -crystallin, which is linked to a desmin-related myopathy, results in an irregular structure and defective chaperone-like function. *Proc Natl Acad Sci USA* 96:6137–6142
- Bruey JM, Ducasse C, Bonniaud P, Ravagnan L, Susin A, Diaz-Latoud C, Gurbuxani S, Arrigo AP, Kroemer G, Solary E, Garrido C (2000) Hsp27 negatively regulates cell death by interacting with cytochrome *c*. *Nat Cell Biol* 2:645–652
- Bukach OV, Seit-Nebi AS, Marston SB, Gusev NB (2003) Some properties of human small heat shock protein Hsp20 (HspB6). *Eur J Biochem* 271:291–302
- Diaz-Latoud C, Buache E, Javouhey E, Arrigo AP (2005) Substitution of the unique cysteine residue of murine Hsp25 interferes with the protective activity of this stress protein through inhibition of dimer formation. *Antioxid Redox Signal* 7:436–445
- Eaton P, Fuller W, Shattock MJ (2002) S-Thiolation of Hsp27 regulates its multimeric aggregate size independently of phosphorylation. *J Biol Chem* 277:21189–21196
- Ecroyd H, Carver JA (2009) Crystallin proteins and amyloid fibrils. *Cell Mol Life Sci* 66:62–81
- Feil IK, Malfois M, Hendle J, van der Zandt H, Svergun DI (2001) A novel quaternary structure of the dimeric alpha-crystallin domain with chaperone-like activity. *J Biol Chem* 276:12024–12029
- Ghosh JG, Clark JI (2005) Insight into the domain required for dimerization and assembly of human  $\alpha B$  crystallin. *Protein Sci* 14:684–695
- Ghosh JG, Shenoy AK, Clark JI (2007) Interactions between regulatory proteins and human  $\alpha B$  crystallin. *Biochemistry* 46:6308–6317
- Haley DA, Bova MP, Huang Q-L, Mchaourab HS, Stewart PL (2000) Small heat-shock proteins structures reveal a continuum from symmetric to variable assemblies. *J Mol Biol* 298:261–272
- Haslbeck M, Franzmann T, Weinfurter D, Buchner J (2005) Some like it hot: the structure and function of small heat shock proteins. *Nat Struct Biol* 12:842–846
- Jehle S, van Rossum B, Stout JR, Noguchi SR, Falber K, Rehbein K, Oschkinat H, Kleivit RE, Rajagopal P (2009)  $\alpha B$ -crystallin: a hybrid solid-solution state NMR investigation reveals structural aspects of the heterogeneous oligomer. *J Mol Biol* 385:1481–1497
- Kasakov AS, Bukach OV, Seit-Nebi AS, Marston SB, Gusev NB (2007) Effect of mutations in the  $\beta 5$ - $\beta 7$  loop on the structure and properties of human small heat shock protein HSP22 (HspB8, H11). *FEBS J* 274:5628–5642
- Kim KK, Kim R, Kim SH (1998) Crystal structure of small heat-shock protein. *Nature* 394:595–599
- Kim MV, Kasakov AS, Seit-Nebi AS, Marston SB, Gusev NB (2006) Structure and properties of K141E mutant of small heat shock protein Hsp22 (HspB8, H11) that is expressed in human neuromuscular disorders. *Arch Biochem Biophys* 454:32–41

- Kim MV, Seit-Nebi AS, Marston SB, Gusev NB (2004) Some properties of human small heat shock protein Hsp22 (H11 or HspB8). *Biochem Biophys Res Commun* 315:796–801
- Kumar LVS, Ramakrishna T, Rao CM (1999) Structural and functional consequences of the mutation of conserved arginine residue in  $\alpha A$  and  $\alpha B$ -crystallins. *J Biol Chem* 274:24137–24141
- Laemmli UK (1970) Cleavage of structural proteins during assembly of the head of bacteriophage T4. *Nature* 227:680–685
- Mchaourab HS, Godar JA, Stewart PL (2009) Structure and mechanism of protein stability sensors: chaperone activity of small heat shock proteins. *Biochemistry* 48:3828–3837
- Michiel M, Skouri-Panet F, Duprat E, Simon S, Ferard C, Tardieu A, Finet S (2009) Abnormal assemblies and subunit exchange of  $\alpha B$ -crystallin R120 mutants could be associated with destabilization of the dimeric substructure. *Biochemistry* 48:442–453
- Mounier N, Arrigo AP (2002) Actin cytoskeleton and small heat shock proteins: how do they interact? *Cell Stress Chaperones* 7:167–176
- Murugesan R, Santhoshkumar P, Sharma KK (2008) Role of  $\alpha B15$  and  $\alpha B162$  residues in subunit interaction during oligomerization of  $\alpha B$ -crystallin. *Mol Vis* 14:1835–1844
- Permyakov EA (1993) Luminescent spectroscopy of proteins. CRC, Boca Raton
- Perng MD, Muchowski PJ, van den Ijssel P, Wu GJS, Hutcheson AM, Clark JI, Quinlan RA (1999) The cardiomyopathy and lens cataract mutation in  $\alpha B$ -crystallin alters its protein structure, chaperone activity, and interaction with intermediate filaments. *J Biol Chem* 274:33235–33243
- Sarkar G, Sommer SS (1990) The megaprimer method of site-directed mutagenesis. *Biotechniques* 8:404–407
- Simon S, Michiel M, Skouri-Panet F, Lechaire JP, Vicart P, Tardieu A (2007) Residue R120 is essential for the quaternary structure and functional integrity of human  $\alpha B$ -crystallin. *Biochemistry* 46:9605–9614
- Sreelakshmi Y, Santhoshkumar P, Bhattacharyya J, Sharma KK (2004)  $\alpha A$ -Crystallin interacting regions in the small heat shock protein,  $\alpha B$ -crystallin. *Biochemistry* 43:15785–15795
- Sreerama N, Woody RW (2000) Estimation of protein secondary structure from circular dichroism spectra: comparison of CONTIN, SELCON, and CDSSTR methods with an expanded reference set. *Anal Biochem* 287:252–260
- Stamler R, Kappe G, Boelens W, Slingsby C (2005) Wrapping the  $\alpha$ -crystallin domain fold in a chaperone assembly. *J Mol Biol* 353:68–79
- Sun Y, MacRae TH (2005) The small heat shock proteins and their role in human disease. *FEBS J* 27:2613–2627
- Taylor RP, Benjamin IJ (2005) Small heat shock proteins: a new classification scheme in mammals. *J Mol Cell Cardiol* 38:433–444
- van Monfort RLM, Basha E, Friedrich KL, Slingsby C, Vierling E (2001) Crystal structure and assembly of eukaryotic small heat shock protein. *Nat Struct Biol* 8:1025–1030
- Vos MJ, Hageman J, Carra S, Kampinga HH (2008) Structural and functional diversities between members of the human HSPB, HSPH, HSPA, and DNAJ chaperone families. *Biochemistry* 47:7001–7011
- Walker JM (2002) Gradient SDS polyacrylamide gel electrophoresis of proteins. In: Walker JM (ed) *The protein protocols handbook*, 2nd edn. Humana, Totowa, pp 69–72
- Zavialov AV, Benndorf R, Ehrnsperger M, Zav'yalov V, Dudich I, Buchner J, Gaestel M (1998a) The effect of the intersubunit disulfide bond on the structure and functional properties of the small heat shock protein Hsp25. *Int J Biol Macromol* 22:163–173
- Zavialov AV, Gaestel M, Korpela T, Zav'yalov VP (1998b) Thiol-disulfide exchange between small heat shock protein 25 and glutathione. *Biochim Biophys Acta* 1388:123–132